Stationarity of the detrended price return in stock markets

Karina Arias-Calluari[a,1], Morteza. N. Najafi[b], Michael Harré[c] and Fernando Alonso-Marroquin[a]

[a]*School of Civil Engineering, The University of Sydney, Australia*

[b]*Department of Physics, University of Mohaghegh Ardabili, Ardabil, Iran*

[c]*Complex Systems Research Group, Faculty of Engineering, The University of Sydney, Australia*

Abstract

This paper proposes a governing equation for stock market indexes that accounts for non-stationary effects. This is a linear Fokker-Planck equation (FPE) that describes the time evolution of the probability distribution function (PDF) of the price return. By applying Ito's lemma, this FPE is associated with a stochastic differential equation (SDE) that models the time evolution of the price return in a fashion different from the classical Black-Scholes equation. Both FPE and SDE equations account for a deterministic part or trend, and a stationary, stochastic part as a q-Gaussian noise. The model is validated using the S&P500 index's data. After removing the trend from the index, we show that the detrended part is stationary by evaluating the Hurst exponent of the multifractal time series, its power spectrum, and its autocorrelation.

1. Introduction

Complex dynamic systems encountered in industry or business [9], financial markets [49, 24], genetics [51], neuroscience [46, 50], biomedicine [30, 13], ocean dynamics [20] and seismology [44] generate non-stationary time series. A time series is non-stationarity when it is non-identically distributed throughout their full length of time [53, 42, 7]. In stock markets, these type of time series are simple price return [49, 7, 40], volatility of index price [58] and trading stock volume [38]. In the statistical analysis of financial markets, the non-stationarity time series that is extensively analyzed is the simple price return, which is an arithmetical difference [38]. For price return, the non-stationarity is produced by the non-constant activity during a trading day and the heterogeneity of market participants [54, 14, 49].

The non-stationary time series are difficult to analyze because the process remains in a non-equilibrium state. Consequently, their models do not achieve optimal forecasting and control [9]. Therefore, it is challenging to obtain an accurate model that can be used to calculate the probability of future value based on initial conditions.

In recent years extensive research has been devoted to model the index price return distributions considering its characteristic features and non-stationarity properties [1, 48, 47]. The Black Scholes equation had been the novel governing equation to describe the characteristics of the stock return distribution [12]. This important model assumes the geometric Brownian motion (GBM) equation to model the Index price return. However, it fails to capture the non-Gaussian properties of the price return [12], negative skewness [1], and negative values obtained from recent events [63]. As a result, different models started to appear, applying modifications or generalizations to the GBM. The fractional Brownian motion (FBM) [3], the mixed fractional Brownian

motion (MFBM) as a combination of the Brownian motion with the FBM [56], the generalized mixed fractional Brownian motion (GMFBM) [27, 59]. These new models capture better the characteristic features of the Index price return. However, they were developed considering a neutral risk assumption [27]. As an alternative to these traditional stock return models, an increasing number of quantum models have also been applied to study the stochastic dynamics of stock prices. The most well-known are; the quantum spatial-periodic harmonic model (QSH) [48], the quantum Brownian motion model (QBM) [47], the quantum harmonic oscillator model (QHO) [1]. An advantage of these models is that they incorporate the market uncertainty (risk), although they have been derived from the stochastic equation of a Brownian process.

In this paper, a new governing equation of non-stationary simple price return is presented. This governing equation is based on a simpler but more effective approach. The time-series is decomposed by a deterministic part or trend and a stochastic part or q-gaussian noise. The stochastic part is stationary and can be modeled by a q-gaussian distribution. To validate our governing equation, the trend of the SP&500 index data is removed by applying a moving average method (MA) based on the Kurtosis evaluation [24]. By applying different tests, it is shown that the detrended price return is a stationary process. Thus, the PDF of the price return obeys the proposed partial differential equation (PDE).

The stationary testing methods include an estimation of a Hurst exponent H, which itself characterizes the self-similarity of the time series [46]. Time series are classified as monofractal or multifractal depending on how the Hurst exponent varies over several orders of magnitude [23]. The monofractal time series posses a unique Hurst exponent. The stationarity test for the monofractal time series is based on its autocorrelation function, where its decay depends directly on the Hurst exponent [34]. The multifractal time series does not have a unique Hurst exponent [36]. The stationarity test for multifractal time series is based on the relation between two sets
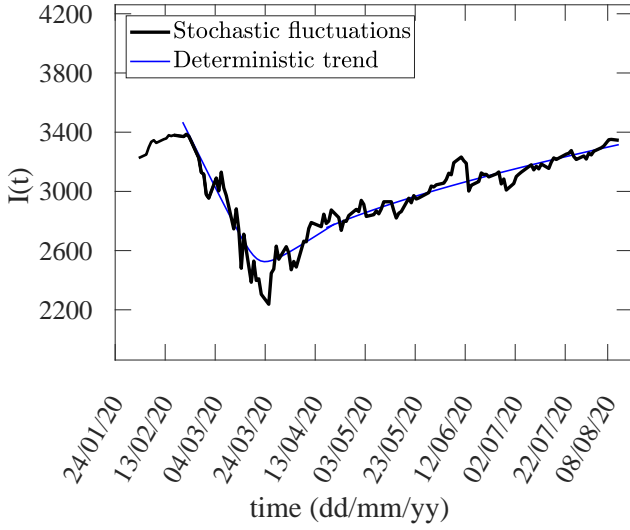
Figure 1: Schematic plot of a downward and upward swing in the S&P500. The index is decomposed into a deterministic trend (blue) and stochastic fluctuations (dotted black).

of scaling exponents obtained from the standard detrending fluctuation analysis (DFA) [40, 34] and the generalized detrending fluctuation analysis (G-DFA) [34, 24], respectively.

This paper is divided into four parts: In Section 2, the governing equation of the simple price return is presented. Section 3 presents a straightforward way to detrend the stock market price, based on the optimization of a moving window via the kurtosis evaluation. In Section 4, we perform two statistical tests on the detrended price return to show that it is stationary. The first test is based on the evaluation of the Hurst exponent in terms of the orders of the statistical moments of the time series. The second test verifies that the power spectrum of the time series equals the Fourier transform of its autocorrelation [64, 31]. Apart from showing that our detrended time series is stationary, we provide the details of the Hurst exponent calculation and the characterization of the detrended price return. Finally, the conclusions and perspectives of this work are presented in Section 5.

2. Governing equation of price return

The conventional approach to option pricing analysis leads to the classical Black-Scholes equation or non-linear Black-Scholes equation (BSE) as the governing equation of price return[8]. A limitation of the BSE is the assumption that stock prices follow a geometric Brownian motion pattern, ignoring that prices can have sustained trends and even can reach negative values in the real indexes [63]. Our governing equation covers BSEs' limitations, allowing the price to fluctuates in a particular direction (trend) and incorporating stationary q-Gaussian noise. The q-Gaussian noise is a better descriptor of the fluctuations in stock markets [4]. For this analysis, the price return at time t is defined as [43, 32, 62]:

$$X(t_0, t) = I(t_o + t) - I(t_o), \quad (1)$$

where $I(t_0)$ is the stock market index at time t_0, and $I(t)$ is the stock market index for any time $t > t_0$.

Our approach decomposes the price return $X(t)$ into a deterministic component $\overline{X}(t)$ and a stationary q-Gaussian noise x,

$$X(t) = \overline{X}(t) + x. \quad (2)$$

In earlier work, we presented the probability density function (PDF) of the detrended price return $x(t)$, described by the functional form [4]:

$$P(x,t) = \frac{1}{(Dt)^{1/\alpha}} \frac{1}{C_q} \left[1 - (1-q)\frac{x^2}{(Dt)^{2/\alpha}} \right]^{\frac{1}{1-q}}, \quad (3)$$

where D, q and α are time-dependent fitting exponents. The normalization constant C_q for $1 < q < 3$ is given by:

$$Cq = \sqrt{\frac{\pi}{q-1}} \frac{\Gamma((3-q)/(2(q-1)))}{\Gamma(1/(q-1))}. \quad (4)$$

Then, we apply the following change of variable $T = t^\xi$, where $\xi = \frac{3-q}{\alpha}$, in the governing equation of $P(x,t)$ [Eq.(12) from [4]]. The corresponding Partial Differential Equation (PDE) is:

$$\frac{\partial P}{\partial T} = D^\xi \frac{\partial^2 P^{2-q}}{\partial x^2}. \quad (5)$$

By applying Eq. (2) the PDF of price return $P(X, T)$ is:

$$P(X,T) = \left(\frac{1}{(DT)^{1/\alpha}} \frac{1}{C_q} \right) \left[1 - (1-q)\frac{[X - \overline{X}(T)]^2}{(DT)^{2/\alpha}} \right]^{\frac{1}{1-q}}. \quad (6)$$

Then, the chain rule is applied to obtain the governing equation of $P(X, T)$.

$$\frac{\partial^2}{\partial^2 x} = \frac{\partial^2}{\partial^2 X}$$
$$\frac{\partial}{\partial T} = \frac{1}{\xi} t^{1-\xi} \frac{\partial}{\partial t} + \frac{\partial \overline{X}(T)}{\partial T} \frac{\partial}{\partial X} \quad (7)$$

By replacing Eq(7) in Eq(5), the general PDE can be defined considering that $\frac{t^{1-\xi}}{\xi} = \frac{\partial t}{\partial T}$ as:

$$\frac{\partial P}{\partial T} = D^\xi \frac{\partial^2 P^{2-q}}{\partial X^2} - \frac{\partial \overline{X}(T)}{\partial T} \frac{\partial P}{\partial X}. \quad (8)$$

The term D^ξ is the diffusive parameter, which is independent on X. Consequently, a comparison between Eq(8) with the linear Fokker-Planck equation (LFPE) is made. The LFPE is :

$$\frac{\partial P(X,T)}{\partial \tau} = -\frac{\partial (D_1 P(X,T))}{\partial x} + \frac{\partial^2 (D_2 P(X,T))}{\partial x^2}, \quad (9)$$

After that, the diffusion coefficient in the LFPE is defined as: $D_2 = D^\xi P(X, T)^{1-q}$. By replacing Eq(6) into this equation, we obtain an explicit expression for diffusion coefficient of the LFPE:

$$D_2 = D^{2/\alpha} C_q^{q-1} T^{(q-1)/(3-q)} \left[1 - \frac{(1-q)[X - \overline{X}(T)]^2}{(D^\xi T)^{2/(3-q)}} \right]$$

(10)

and the drift term is:

$$D_1 = \frac{\partial \overline{X}(t)}{\partial T}$$

(11)

The drift term is the overall direction of the index price (trend), and it shows particular tendencies. It is associated with the systematic risk response, where external events can produce a change of trend direction [5]. This feature implies that future price changes are dependent on the past values and therefore it is possible to develop a forecast in the short term with some degree of confidence.
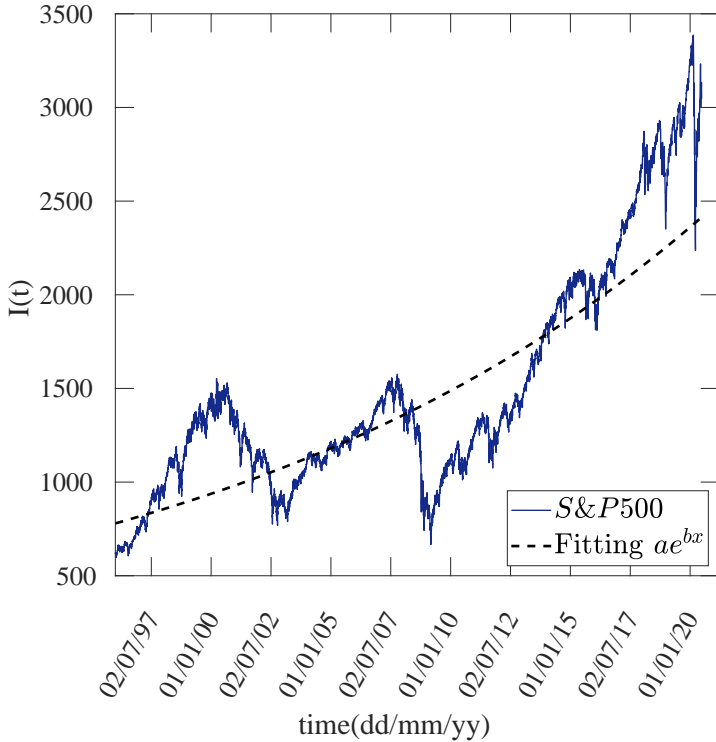

Figure 2: (Stock market index $I(t)$ of S&P500 in the period of 02/01/96 to 30/06/20 (24 years). Considering the GBM in Eq. (13), the deterministic part is modeled to find the trend of the S&P500. As a result, the fitted line ae^{bx} is an approximation of the S&P500 data trend, where $a = 7.45(10^{-38}) \pm 5.97(10^{-39})$ and $b = 0.0001264 \pm 10^{-07}$. However, if this approximated trend is subtracted, the fluctuations will form a not stationary time series because their statistical properties will change on time.

The Fokker-Planck equation in Eq. (9) is used to obtain the probability distribution of price return at any time. The stochastic differential equation (SDE) represents the dynamics of price return as a function of time [61]. The SDE can be obtained by applying Ito Lemma [61] in Eq.(9):

$$dX_T = \mu(T)dT + \sigma(X, T)dW_T,$$

(12)

with drift $\mu(T) = D_1(T)$ and variance $\sigma^2(X, T) = 2D_2(X, T)$. The function W_T is the q-Gaussian noise. The interpretation of our SDE is that in a small time interval, dT, the price return changes its value due two effects: the first one is related with the drift D_1 that depends on time only. The second is the diffusion term D_2 that depends on time and price return. The SDE in Eq. (12) is different from the Geometrical Brownian Motion (GBM) [60]:

$$dI_T = \mu I_T dT + \sigma I_T dB_T,$$

(13)

where, μ and σ values are constants, and B_T is the standard Brownian noise. The GBM is the basic model for stock price dynamics in the Black-Scholes framework[61]. If we consider the approximation, $Z_T = dI_T/I_T$, where Z_T is a logarithmic difference of the stock market index $Z(t_0, t) = \ln\left[\frac{I(t_0+t)}{I(t_0)}\right]$. Then, Eq. (13) can be simplified as $Z_T = \mu dT + \sigma dB_T$. The solution of this equation is an exponential growth superposed by a normally distributed Brownian process [61]. This solution constitutes a rough approximation of the price return, as shown in Figure 2. In some studies, the log-return Z_T is often used for technical analysis because it is close to the percentage price change [57, 11], a concept often used to neutralize most of the non-stationary effects [21, 41, 15, 33].

One of the key properties of the GBM approach to modeling asset prices is that prices will not go negative, an assumption that may not be reasonable given recent events in some asset markets. Some examples are crude oil's price fall and the bankruptcy of some assets of global energy companies, which had reached negative values [63]. Additionally, in the GBM, it is assumed that the natural logarithmic of price return follows the Brownian motion with drift and that the price return has a normal distribution [61]. However, price returns or log price returns have been modeled by a q-Gaussian distribution function [65]. Thus, the stochastic differential equation, Eq.(12), could potentially model this behavior better than the standard GBM.

In what follows, we present an analysis of the S&P500 index per minute for the past 24 years in the time frame of 1996-2020 as a case study to decompose the time series into a deterministic trend and a stationary stochastic part. The S&P500 stock market index data was obtained from the Thomson Reuters Corporation [16]. Before the analysis, few artifacts were removed from the data [17, 52, 18], as explained in the Appendix A.

3. Detrending time series

The Moving Average is a widely known method to remove the trend in a time series [26, 24, 4]. Many variations

and implementations have been developed by researchers, but its underlying purpose remains, which is to determine the trend. Despite new models, the MA method is still considered as a good option for detrending the data due to its easiness, objectiveness, reliability, and usefulness [26].

The MA is a common average within a time window size that is shifted forward until the end of the data set [26]. Each point in the time series data is equally weighted. The arithmetic centered moving average has been the most widely used MA case [45].

The MA method offers different options for its calculation. The first option is regarding how the time window will be shifted until the end of the data. For this analysis, it has been used an overlapped or rolling window. These windows are extended over an interval $[t, \ t + t_w]$, where the consecutive window is incremented by one time point to: $[t+1, \ t+t_w+1]$. The t_w represents the size of the time window. The second option is choosing the polynomial order k for fitting each time segment for the detrending process. The original MA uses $k = 0$, which represents an unweighted mean [51]. The option $k = 1$ is used in other studies when the focus is on the local trend (particular tendency per window) [2]. These options were tested and applied in the index price $I(t)$. In our analysis, there is no major difference between $k = 0$ and $k = 1$, so that $k = 0$ was used.

3.1. Optimal time window

The size of the time window, t_w, is the key parameter to obtain stationary detrended data. The distribution of the data set of each window t_w should be similar, without outliers (extreme events) to achieve an equilibrium state of the dynamic system [65]. Xu et al.[65] applied the kurtosis definition to compare each distribution of the data set of each window t_w. The kurtosis is defined as the fourth standardized moment, defined as the relation between central moments $\langle u^n \rangle$ of order n,

$$K = \frac{\langle u^4 \rangle}{\langle u^2 \rangle^2}, \tag{14}$$

where the delimiters $\langle \ \rangle$ denotes time average for each particular window.

The optimal time window must satisfy the condition of $K \approx 3$, to obtain a distribution, in which extreme or outlier events are very unlikely to occur [10, 65].
Before applying the MA method, we developed a preliminary process to choose an optimal time window t_w. We used a range of values between 1 to 25 months as a possible time window. For each possible t_w value, the total length of N of the time series is split into non-overlapping time windows. The total length of N is often not a multiple of the time window, t_w. Consequently, the number of segments is defined by rounding them to the nearest lower integer $\lfloor n = N/t_w \rfloor$. Next, the kurtosis in each jth window is calculated, where $j = 1, 2, 3, 4.....n$. and averaged for the n windows as follows;
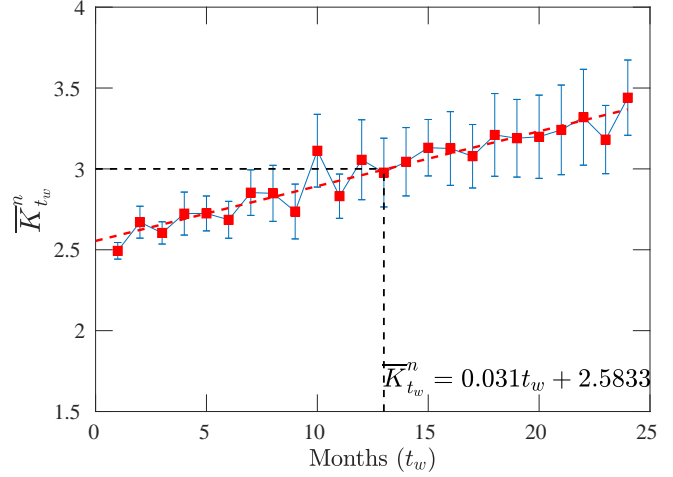

Figure 3: Optimal window size t_w that will be used for the Moving Average. The $\overline{K}_{tw}^{n} = 3$ yields a time window of 13 ± 1 months. In order to have an integer unit for t_w , t_w = 12 months was chosen. The blue bars are graphical representations of the standard error of $\overline{K}_{tw}^{n}$ data in average per t_w

$$\overline{K}_{t_w}^{n} = \frac{1}{n} \sum_{j=1}^{n} K_{t_w}(j), \tag{15}$$

where $\overline{K}_{t_w}^{n}$ denotes the average over the n windows. Figure 3 presents the results of $\overline{K}_{t_w}^{n}$. The optimal window size is 13 ± 1 months. The time window assumed for the MA analysis is 12 months. The smaller value of time window, t_w, is chosen because it will preserve features of the data such as peak height and width, which is usually attenuated with a longer time window t_w.

3.2. Calculation of trend and fluctuating part

The non-stationary time series of the stock market index $I(t)$ is splited into a trend $\tilde{I}(t)$ and a stationary fluctuating component $I^*(t)$,

$$I^*(t) = I(t) - \tilde{I}(t). \tag{16}$$

The trend $\tilde{I}(t)$ is constructed for the index price of S&P500 applying MA method with $k = 0$ and considering overlapped windows of $t_w = 12$ months. This process is constructed based on a weighted sum or average of each time window. There are three cases to calculate the moving average that depends on the position of the moving window [24]:

- For $t < \frac{t_w}{2}$

$$\tilde{I}(t) = \frac{1}{t_w} \sum_{k=-\lfloor (t-1) \rfloor}^{\lfloor (t_w-1)/2 \rfloor} I(t + k) \tag{17}$$

- For $\frac{t_w}{2} < t < N - \frac{t_w}{2}$

$$\tilde{I}(t) = \frac{1}{t_w} \sum_{k=-\lfloor (t_w-1)/2 \rfloor}^{\lceil (t_w-1)/2 \rceil} I(t+k) \qquad (18)$$

- For $t > N - \frac{t_w}{2}$

$$\tilde{I}(t) = \frac{1}{t_w} \sum_{k=-\lfloor (t_w-1)/2 \rfloor}^{\lceil N-t \rceil} I(t+k), \qquad (19)$$

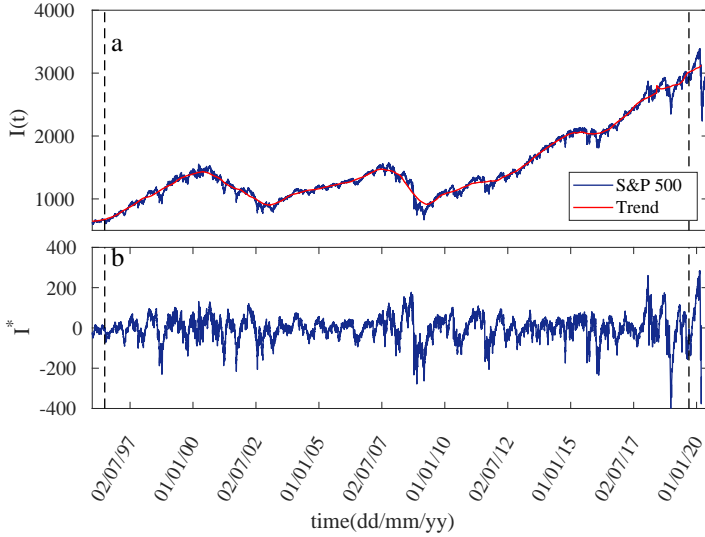with the time step of $t = 1, 2, 3....N$ for the index fluctuations.

Figure 4: (a) Trend obtained after applied the MA analysis for a time window of 12 months for S&P 500 data. (b) Detrend price $I^*(t)$ after subtracting the trend shown on subfigure 4-a.

Figure 4a presents the trend $\tilde{I}(t)$ after applying the MA analysis for a time window of 12 months. The trend obtained represents a general tendency of the stock market index $I(t)$. The Figure 4b shows the detrended price as a result of subtracting the obtained trend.

4. Stationarity of detrended price return

In the following section, we test the detrended time series for stationarity. These tests are based on the calculation of the Hurst exponent and the power spectrum analysis, respectively. The detrended price return is defined as,

$$x(t) = I^*(t_o + t) - I^*(t_o), \qquad (20)$$

where $I^*(t_o)$ is the detrended stock market index at time t_o, and $I^*(t)$ is the detrended stock market index for any time $t > t_o$.

4.1. First stationary test

For this test, the Hurst exponent of this time series is calculated. This Hurst exponent is a measure of long-range memory of a time series. More specifically, it measures the statistical dependence of two points of the time series with respect to the time difference between them [36]. The Hurst exponent is better known as the *index of dependence*, and as such, it is a dimensionless estimator of self-similarity in a time series [46, 28]. The self-similarity occurs when a structure repeats itself on subintervals, so they are *scale-invariant*, which is a property that some time series posses [46]. Two types of self-similar signals exist. The monofractal signal, which presents a unique scaling behavior of complexity. The scaling behavior is obtained from the ratio of the self-similar pattern that changes with the scale at which it is measured. The second type is the multifractal signal, which has more than one scaling behavior [29].

The Hurst exponent is estimated by applying the detrended fluctuation analysis (DFA) [29] explained in the Appendix B. The DFA is a technique to demonstrate self-similarity in a time series [6]. The DFA method provides complementary information, such as the Hurst exponent. Additionally, by analyzing the statistics, it is possible to characterize the time series as monofractal or multifractal if the self-similarity exists.

The first part of the DFA analysis consists in removing the trend of the original time series considering non-overlapping segments. However, our trend was removed by applying a simple but still rigorous MA method considering overlapped time windows with an optimal size of time window t_w.

The DFA is based on the calculations of the *statistical moments*, $F_w(s)$, as a function of the *time segment s*, where w is the order of the moment [51, 39, 2]. The full definition is given in Eq.(26) in the Appendix B. If the time series satisfies the $F_w(s) \sim s^H$, the time series is monofractal, and the exponent H is called the Hurst exponent [36, 35]. Other time series do not have a unique, constant valued H. Their scaling exponent H depends on the order of the moment w (Figure B.1). These are classified as a multifractal time series. The generalization method of DFA (G-DFA) is tailored for multifractal time series. In the G-DFA, the *generalized statistical moments* are defined by $G_w(s)$ in Eq. (31). If the series is multifractal, the exponent $\tau(w)$ is the so-called *generalized scaling exponent* (GSE). The multifractal time series satisfies the scaling law of $G_w(s) \sim s^{\tau(w)}$. For stationary and normalized multifractal time series the generalized scaling exponent $\tau(w)$ can be defined in terms of the generalized Hurst exponent $h(w)$ [34]:

$$\tau(w) = wh(w) - 1. \qquad (21)$$

The Figure 5a shows the generalized Hurst exponent obtained from Figure B.1, and its fitting. The generalized Hurst exponent is approximated to $h(w) \simeq -0.023w + 0.521$ for $-5.0 \leq w \leq 5.0$. Figure 5b shows the $\tau(w) = wh(w) - 1$ relationship, proving that the detrended price return is stationary and multifractal [34].
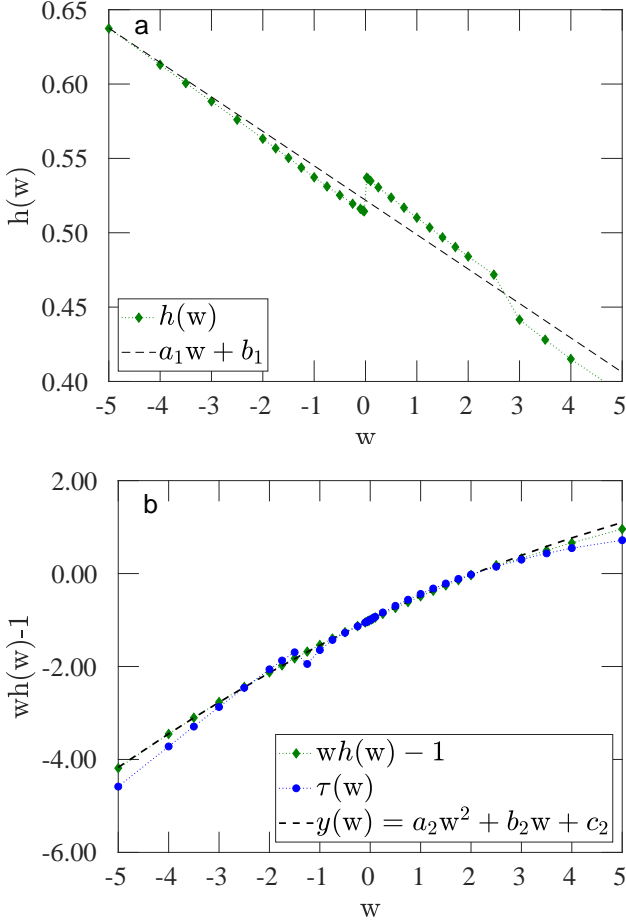
Figure 5: Evaluation of the scale exponents, $h(w)$, and the generalized scaling exponent, $\tau(w)$, obtained from results shown in Figure B.1 and B.2 respectively. The generalized Hurst exponent $h(w)$ follows Eq. (21) for a normalized and multifractal time series.(a) For the fitting of the generalized Hurst exponent $a_1 = -0.0232 \pm 0.002$ and $b_1 = 0.5219 \pm 0.004$ (b) For the fitting of the generalized scaling exponent $a_2 = -0.02157 \pm 3.8(10^{-4})$, $b_2 = 0.527 \pm 0.0012$, $c_2 = -0.9954 \pm 0.0034$

4.2. Second stationary test

This test is presented to prove stationary without using the Hurst exponent. This test is based on the autocorrelation and the power spectrum analysis of the time series, by applying the stationary definition [64].

First, we proceed to evaluate the correlation of the detrended price return [36, 19, 34, 55]. The autocorrelation is defined as;

$$C_x(s) \equiv \frac{\langle x_t x_{t+s} \rangle}{\sigma_x^2}, \qquad (22)$$

$$\sigma_x^2 = \langle (x_t - \mu)(x_t - \mu) \rangle.$$

The presence of short-time autocorrelations is shown in Figure 6, where the detrended price return for a specific time is

represented by x_t. The power-law fitting of the autocorrelation holds only one order of magnitude. For lower values of s, the autocorrelation has an exponential trend, and higher values show a weak but non-zero correlation. A transition zone is observed between lower and higher time-lag values, and it decreases rapidly with a power law that has an exponent $\gamma = -1.02 \pm 0.52$.
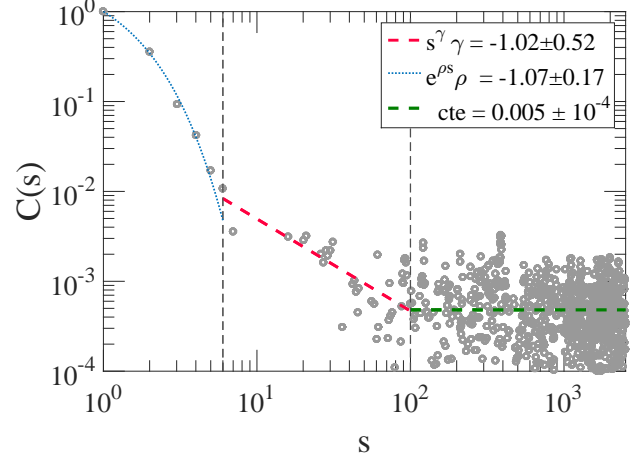

Figure 6: Autocorrelation of the detrended price return calculated as $C_x(s) \equiv \dfrac{\langle x_t x_{t+s} \rangle}{\sigma_x^2}$. Short-time correlations are observed for the first 6 minutes. A weak long-time correlation appears after 100 minutes.
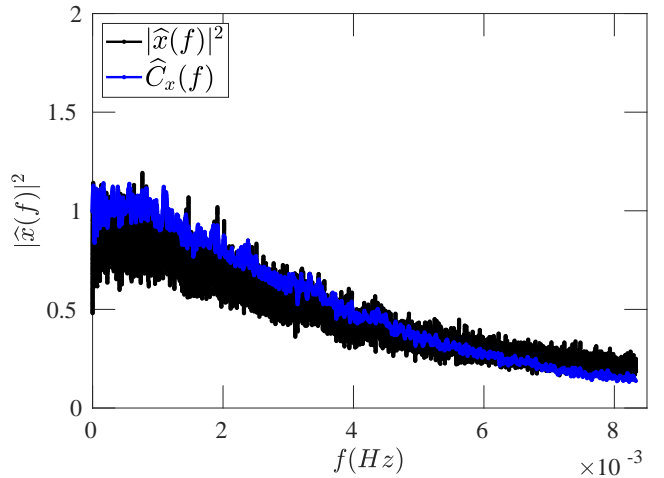

Figure 7: The Power-spectral density $|\hat{x}(f)|^2$ of the detrended price return matches with the Fourier transform of its autocorrelation.

Then, we represent $\hat{x}(f)$ as the Fourier Transformation (FT) of x_t.

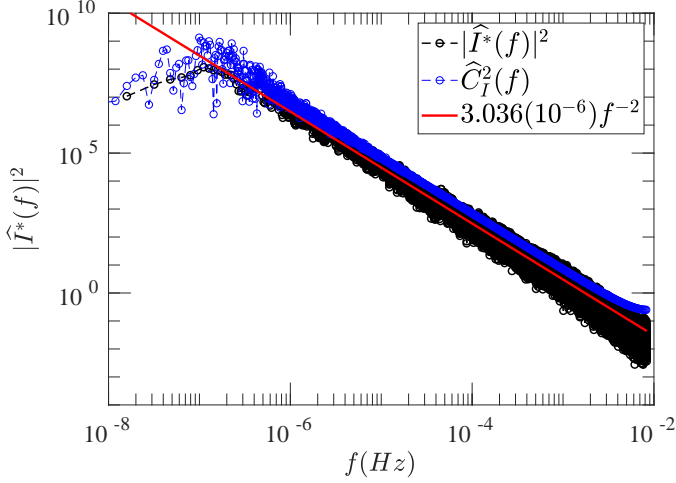$$\hat{x}(f) = \frac{1}{\sqrt{T}} \sum_{t=0}^{T} x(t) e^{-2\pi i f t}. \qquad (23)$$

Figure 8: The power-spectral density of the detrended index $I^*(t)$ holds a power law $P(f) = M/f^2$, where $M = 3.036(10^{-6}) \pm 3(10^{-9})$. The following relation $|\widehat{I}(f)|^2 = \widehat{C}_I^2(f)$ is observed, suggesting that the Index once detrended is stationarity as well.

This test states that any process is stationary if the power spectrum $|\widehat{x}(f)|^2$ exists, and can be expressed as the Fourier transform of the autocorrelation $C(s)$ [64, 37],

$$|\widehat{x}(f)|^2 = \widehat{C}_x(f), \tag{24}$$

We determine that the detrended price return is a stationarity time series based on the results shown in Figure 7, where the match between $|\widehat{x}(f)|^2$ and $\widehat{C}_x(f)$ is achieved. The $|\widehat{x}(f)|^2$ and the $\widehat{C}_x(f)$ have been smoothed by applying the Savitzky-Golay filtering. The smoothed is made with the purpose of reducing the noise of the data without distorting their tendency [25, 22]. The smoothing obtained by the Saviztky-Golay filter is based on the least-squares of a linear fitting across a moving window by applying the normalized convolution integers of Savitzky-Golay, C_i [25, 22]. For this case the length of the moving window is $3.97(10^{-5})$ Hz. Also, the relation $|\widehat{I}(f)|^2 = \widehat{C}_I^2(f)$ is observed in Figure 8, suggesting the profile of the detrended price return is stationary too. From this test, we can conclude once again that the detrended price return is a stationary time series.

5. Conclusions

To conclude, the S&P500 index was detrended using a weighted average method with an overlapped time window of one year. Two independent tests demonstrated that the detrended price return is a multifractal, stationary time series with short-time correlations.

The two independent tests that prove stationarity of the detrended price return were: (1) The generalized scaling exponent $\tau(w)$ can be expressed in terms of the general form of the Hurst exponent $h(w)$, and (2) the power spectrum of the time series is approximately equal to the Fourier transform

of its autocorrelation. These tests validated our improved version of the Black-Scholes equations postulated at the beginning of our paper.

The governing equations proposed in this paper remove the limitation of the classical Black-Scholes equation and its modifications. By proposing a simpler and more effective approach, the new governing equations can describe the price return and its characteristics features. The proposed SDE in Eq. (12) presents its deterministic component as endogenous or exogenous predictive factors, which is associated with internal/external events that produce changes of trend direction. The stochastic part is represented by the q-Gaussian noise. Our stochastic differential equation captures the index behavior more precisely by having a trend that fluctuates deterministically. Then, the detrended part is presented as a stationarity time series. Future work should be focused on the analysis of the fractional Fokker-Planck Equation (FFPE) to model anomalous fluctuations of the stock market indexes. A wide range of q-Gaussian and the Levy-Stable distribution functions can be obtained to model the stochastic fluctuations after applying the different definitions of the fractional derivatives available in the market.

References

[1] Ahn, K., Choi, M., Dai, B., Sohn, S., Yang, B., 2018. Modeling stock return distributions with a quantum harmonic oscillator. EPL (Europhysics Letters) 120, 38003.

[2] Alessio, E., Carbone, A., Castelli, G., Frappietro, V., 2002. Second-order moving average and scaling of stochastic time series. The European Physical Journal B-Condensed Matter and Complex Systems 27, 197–200.

[3] Ali, A.H., AL-Qazaz, Q.N.N., 2020. Fractional brownian motion inference of multivariate stochastic differential equations. Periodicals of Engineering and Natural Sciences 8, 464–480.

[4] Alonso-Marroquin, F., Arias-Calluari, K., Harré, M., Najafi, M.N., Herrmann, H.J., 2019. Q-gaussian diffusion in stock markets. Physical Review E 99, 062313.

[5] Arias-Calluari, K., Alonso-Marroquin, F., Najafi, M.N., Harré, M., 2020. Forecasting the effect of covid-19 on the s&p500. arXiv preprint arXiv:2005.03969 .

[6] Ausloos, M., 2012. Generalized hurst exponent and multifractal function of original and translated texts mapped into frequency and length time series. Physical Review E 86, 031108.

[7] Bahri, F., Sharples, J., . Sensitivity of the empirical mode decomposition to interpolation methodology and data non-stationarity. Environmental Modeling & Assessment , 1–20.

[8] Barles, G., Soner, H.M., 1998. Option pricing with transaction costs and a nonlinear black-scholes equation. Finance and Stochastics 2, 369–397.

[9] Box, G.E.P., 2013. Time series analysis : forecasting and control. Wiley Series in Probability and Statistics. 4th ed. ed., Wiley, Hoboken.

[10] Buonocore, R., Brandi, G., Mantegna, R., Di Matteo, T., 2019. On the interplay between multiscaling and stock dependence. Quantitative Finance , 1–13.

[11] Cao, W., Hurvich, C., Soulier, P., 2017-09. Drift in transactionâĂŘlevel asset price models. Journal of Time Series Analysis 38, 769,790.

[12] Chen, W., Yan, B., Lian, G., Zhang, Y., 2016. Numerically pricing american options under the generalized mixed fractional brownian motion model. Physica A: Statistical Mechanics and its Applications 451, 180–189.

[13] Chua, K.C., Chandran, V., Acharya, U.R., Lim, C.M., 2010. Application of higher order statistics/spectra in biomedical signalsâĂŤa review. Medical engineering & physics 32, 679–689.

[14] Clara-Rahola, J., Puertas, A.M., Sanchez-Granero, M.A., Trinidad-Segovia, J.E., de las Nieves, F.J., 2017. Diffusive and arrestedlike dynamics in currency exchange markets. Physical review letters 118, 068301.

[15] Cont, R., Tankov, P., 2004. Financial modelling with jump processes. Chapman & Hall CRC, Boca Raton Fla.

[16] Corporation, T.R., 2020. Products and services/news and data. URL: https://www.thomsonreuters.com/en/contact-us.html.

[17] Corporation, Z.I., 24/04/2012. A history of market crashes. URL: https://www.zeninvestor.org/history-market-crashes/.

[18] Ferreira, S., Karali, B., 2015. Do earthquakes shake stock markets? PloS one 10, e0133319.

[19] Gao, J., Cao, Y., Lee, J.M., 2003. Principal component analysis of $1/f\alpha$ noise. Physics Letters A 314, 392–400.

[20] Gay-Balmaz, F., Holm, D.D., 2018. Stochastic geometric models with non-stationary spatial correlations in lagrangian fluid flows. Journal of nonlinear science 28, 873–904.

[21] Gopikrishnan, P., Plerou, V., Amaral, L.A.N., Meyer, M., Stanley, H.E., 1999. Scaling of the distribution of fluctuations of financial market indices. Physical Review E 60, 5305.

[22] Gorry, P.A., 1990. General least-squares smoothing and differentiation by the convolution (savitzky-golay) method. Analytical Chemistry 62, 570–573.

[23] Gu, G.F., Zhou, W.X., 2006. Detrended fluctuation analysis for fractals and multifractals in higher dimensions. Physical Review E 74, 061104.

[24] Gu, G.F., Zhou, W.X., et al., 2010. Detrending moving average algorithm for multifractals. Physical Review E 82, 011136.

[25] Guiñón, J.L., Ortega, E., García-Antón, J., Pérez-Herranz, V., 2007. Moving average and savitzki-golay smoothing filters using mathcad. Papers ICEE 2007, 1–4.

[26] Hansun, S., 2013. A new approach of moving average method in time series analysis, in: 2013 Conference on New Media Studies (CoNMedia), pp. 1–4.

[27] He, X., Chen, W., 2014. The pricing of credit default swaps under a generalized mixed fractional brownian motion. Physica A: Statistical Mechanics and its Applications 404, 26–33.

[28] Horvatic, D., Stanley, H.E., Podobnik, B., 2011. Detrended cross-correlation analysis for non-stationary time series with periodic trends. EPL (Europhysics Letters) 94, 18007.

[29] Hu, K., Ivanov, P.C., Chen, Z., Carpena, P., Stanley, H.E., 2001. Effect of trends on detrended fluctuation analysis. Physical Review E 64, 011114.

[30] Huang, W., Shen, Z., Huang, N.E., Fung, Y.C., 1998. Engineering analysis of biological variables: an example of blood pressure over 1 day. Proceedings of the National Academy of Sciences 95, 4816–4821.

[31] Ivanov, P.C., Ma, Q.D., Bartsch, R.P., Hausdorff, J.M., Amaral, L.A.N., Schulte-Frohlinde, V., Stanley, H.E., Yoneyama, M., 2009. Levels of complexity in scale-invariant neural signals. Physical Review E 79, 041920.

[32] Johnson, N.F., Jefferies, P., Hui, P.M., 2003. Financial market complexity. Oxford University Press, Oxford.

[33] Jondeau, E., Poon, S.H., Rockinger, M., 2007. Financial Modeling Under Non-Gaussian Distributions. Springer Finance, Springer London, London.

[34] Kantelhardt, J.W., Ashkenazy, Y., Ivanov, P.C., Bunde, A., Havlin, S., Penzel, T., Peter, J.H., Stanley, H.E., 2002a. Characterization of sleep stages by correlations in the magnitude and sign of heartbeat increments. Physical Review E 65, 051908.

[35] Kantelhardt, J.W., Koscielny-Bunde, E., Rego, H.H., Havlin, S., Bunde, A., 2001. Detecting long-range correlations with detrended fluctuation analysis. Physica A: Statistical Mechanics and its Applications 295, 441–454.

[36] Kantelhardt, J.W., Zschiegner, S.A., Koscielny-Bunde, E., Havlin, S., Bunde, A., Stanley, H.E., 2002b. Multifractal detrended fluctuation analysis of nonstationary time series. Physica A: Statistical Mechanics and its Applications 316, 87–114.

[37] Krenk, S., Madsen, H.O., Madsen, P.H., 1983. Stationary and transient response envelopes. Journal of Engineering Mechanics 109, 263–277.

[38] Lan, B.L., Yeoh, E.V., Ng, J.A., 2010. Distribution of detrended stock market data. Fluctuation and Noise Letters 9, 245–257.

[39] Liu, Y., Gopikrishnan, P., Stanley, H.E., et al., 1999. Statistical properties of the volatility of price fluctuations. Physical review e 60, 1390.

[40] Maganini, N.D., Da Silva Filho, A.C., Lima, F.G., 2018. Investigation of multifractality in the brazilian stock market. Physica A: Statistical Mechanics and its Applications 497, 258–271.

[41] Mandelbrot, B.B., 1997. Fractals and scaling in finance: discontinuity, concentration, risk : selecta volume E. Springer, New York.

[42] Mandelbrot, B.B., Hudson, R.L., 2010. The (mis) behaviour of markets: a fractal view of risk, ruin and reward. Profile books.

[43] Mantegna, R.N., Stanley, H.E., 1995. Scaling behaviour in the dynamics of an economic index. Nature 376, 46.

[44] Marano, G.C., 2019. Non-stationary stochastic modulation function definition based on process energy release. Physica A: Statistical Mechanics and its Applications 517, 280–289.

[45] Marathe, R.R., Ryan, S.M., 2005. On the validity of the geometric brownian motion assumption. The Engineering Economist 50, 159–192.

[46] Márton, L., Brassai, S., Bakó, L., Losonczi, L., 2014. Detrended fluctuation analysis of eeg signals. Procedia Technology 12, 125–132.

[47] Meng, X., Zhang, J.W., Guo, H., 2016. Quantum brownian motion model for the stock market. Physica A: Statistical Mechanics and its Applications 452, 281–288.

[48] Meng, X., Zhang, J.W., Xu, J., Guo, H., 2015. Quantum spatial-periodic harmonic model for daily price-limited stock markets. Physica A: Statistical Mechanics and its Applications 438, 154–160.

[49] Nava, N., Di Matteo, T., Aste, T., 2016. Time-dependent scaling patterns in high frequency financial data. The European Physical Journal Special Topics 225, 1997–2016.

[50] Oliveira Filho, F., Cruz, J.L., Zebende, G., 2019. Analysis of the eeg bio-signals during the reading task by dfa method. Physica A: Statistical Mechanics and its Applications 525, 664–671.

[51] Peng, C.K., Buldyrev, S.V., Havlin, S., Simons, M., Stanley, H.E., Goldberger, A.L., 1994. Mosaic organization of dna nucleotides. Physical review e 49, 1685.

[52] plummets, M., 20/03/2000. Shares fall more than 60 percent on earnings, revenue restatement. URL: https://money.cnn.com/2000/03/20/companies/microstrategy/.

[53] Politi, M., Millot, N., Chakraborti, A., 2012. The near-extreme density of intraday log-returns. Physica A: Statistical Mechanics and its Applications 391, 147–155.

[54] Ponta, L., Trinh, M., Raberto, M., Scalas, E., Cincotti, S., 2019. Modeling non-stationarities in high-frequency financial time series. Physica A: Statistical Mechanics and its Applications 521, 173–196.

[55] Rangarajan, G., Ding, M., 2000. Integrated approach to the assessment of long range correlation in time series data. Physical Review E 61, 4991.

[56] Rao, B.P., 2016. Pricing geometric asian power options under mixed fractional brownian motion environment. Physica A: Statistical Mechanics and its Applications 446, 92–99.

[57] Ren, L., Ren, P., Glasure, Y., 2018. On the different forms of returns from moving average buy-sell trading rule in the stock market. Benchmarking: An International Journal 25, 253–258.

[58] Roman, H., Porto, M., Dose, C., 2008. Skewness, long-time memory, and non-stationarity: application to leverage effect in financial time series. EPL (Europhysics Letters) 84, 28001.

[59] Thäle, C., 2009. Further remarks on mixed fractional brownian motion. Applied Mathematical Sciences 38, 1885–1901.

[60] Tsay, R.S., 2005. Analysis of Financial Time Series. John Wiley & Sons, Inc., Hoboken, NJ, USA.

[61] Vasconcelos, G.L., 2004. A guided walk down wall street: an introduction to econophysics. Brazilian Journal of Physics 34, 1039–1065.

[62] Voit, J., 2005. The statistical mechanics of financial markets. Third ed., Springer, New York;Berlin;.

[63] Walker, A., 2020. Us oil prices turn negative as demand dries up. URL: https://www.bbc.com/news/business-52350082}:~:text=The%20price%20of%20US%20oil,world%20have%20kept%20people%20inside.

[64] Witt, A., Kurths, J., Pikovsky, A., 1998. Testing stationarity in time series. physical Review E 58, 1800.

[65] Xu, D., Beck, C., 2016. Transition from lognormal to $\chi 2$-superstatistics for financial time series. Physica A: Statistical Mechanics and its Applications 453, 173–183.

A. Appendix A: Cleansing Data

The three artifacts removed from the S&P500 data are: In 17/06/1997, at the peak of the Asian financial crisis [17]. In 20/03/2000, when the imminent bankruptcy of many Internet companies was announced [52]. The third artifact removed was the Haiti earthquake that occurred on 11/01/2010 [18]. These three events introduce spurious jumps in the S&P500, producing a considerable percentage change of the Index for 1 to 8 minutes only. Then, the abrupt Index values return to the original. The three artifacts are shown in Figure A.1(a-c) in chronological order.

B. Appendix B: Detrended Fluctuation Analysis (DFA)

The Detrended Fluctuation Analysis method has become a widespread technique to determine the self-similarity of a time series based on statistical functions F_w [51, 36]. The statistical functions F_w [Eq. (26)] are calculated based on central moments of the time series. For that, the detrended time series is divided into equal non-overlapping segments with a length of s. The s value represents the time segment in which the detrended time series will be analyzed.

Then, the Hurst exponent is obtained from the power law given by F_w vs s.[51, 36, 35].

B.0.1. Description of the method of DFA

We will proceed to indicate the steps to adopt this method to find the Hurst exponent of the detrended price return $x(t)$. First, we focus on calculating the statistical functions F_w, then to the calculation of Hurst exponent H [36, 19, 64, 35, 28].

- *Step 1:* The 'profile' is the cumulative sum of the time series to analyze. For this case, our profile matches with the detrended price $I^*(t)$ obtained after applying Eq. (16).

- *Step 2:* The profile $I^*(t)$ is divided into non-overlapping segments $\lfloor N_s = N/s \rfloor$ with the same length s.
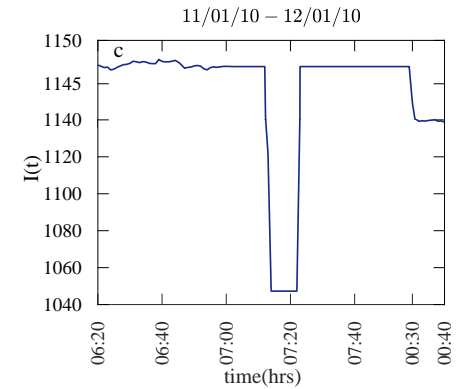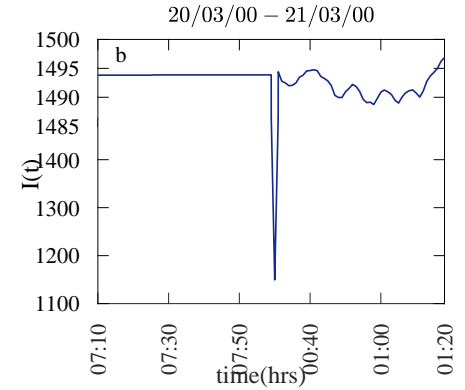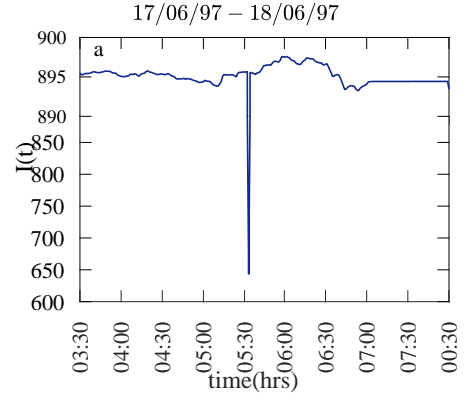

Figure A.1: The three events that produce spurious jumps in S&P500 data over the past 24 years are shown in subfigures (a) the peak of the Asian financial crisis, (b) The imminent bankruptcy of many Internet companies was announced, and (c) The Haiti earthquake effect.

- *Step 3:* The variance for each of the segments $v = 1, 2, 3....N_s$ is obtained by applying the following equation,

$$F^2(v, s) = \frac{1}{s} \sum_{i=1}^{s} (I^*[(v - 1)s + i] - \overline{I^*}(v))^2, \quad (25)$$

where, $\overline{I^*}(v)$ represents the mean of each segment of $I^*(t)$.

- *Step 4:* The statistical moments are obtained considering a range of values for the wth orders.

$$F_w(s) = \left\{ \frac{1}{N_s} \sum_{i=1}^{N_s} [F^2(v, s)]^{w/2} \right\}^{1/w} \quad (26)$$

For detrended time series that present long-range correlations, the following power law is obtained [36, 19, 34, 55]:

$$F_w(s) \sim s^{h(w)}. \quad (27)$$

For monofractal time series $h(w)$ is independent from w value due to a constant scaling behaviour over all the segments ($F^2(v, s)$ in Eq. (25) is cte.) [40, 36], so $H = h(w)$. Figure B.1 shows the results of DFA analysis, where a power law between F_w vs. s is observed. However, the power laws depend on the wth order. Consequently, the Multifractal Detrending Fluctuation Analysis (MF-DFA) is applied to evaluate the dependence between the power laws and the order degree wth.

For a standard multifractal analysis (MF-DFA) the scaling exponent $\tau(w)$ needs to be obtained. This exponent is the power law defined between the $G_w(s)$ vs s. The $G_w(s)$ is a general statistical moment based on the following relationship:

$$G_w(s) = \sum_{v=1}^{N/s} |I^*(vs) - I^*((v - 1)s)|^w, \quad (28)$$

where the term $I^*(vs) - I^*((v - 1)s)$ is equal to the cumulative summation of the $x(t)$ within each segment v of size s.

$$\sum_{t=(v-1)s+1}^{vs} x_t = I^*(vs) - I^*((v - 1)s). \quad (29)$$

In the standard multifractal formalism this sum is better known as the "box probability" $p_s(v)$, and it is used to find hypothetical probability values on the original profile $I^*(t)$.

$$p_s(v) = \sum_{t=(v-1)s+1}^{vs} x_t. \quad (30)$$

Then, by replacing Eq. (30) in Eq. (29). The "box probability" is defined in terms of the original profile, $p_s(v) = I^*(vs) - I^*((v - 1)s)$. After that, we replace this equivalence in Eq. (28), the following relation is obtained:

$$G_w(s) = \sum_{v=1}^{N/s} |p_s(v)|^w, \quad (31)$$

where,

$$G_w(s) \sim s^{\tau(w)}. \quad (32)$$

The $\tau(w)$ represents the classical multifractal scaling exponent, and is related with $h(w)$ for stationary and normalized time series [40, 36],

$$\tau(w) = wh(w) - 1. \quad (33)$$

The Figure 5, shows a summary of the scaling exponents $h(w)$ and $\tau(w)$, respectively. The relationship between $h(w)$ and $\tau(w)$ is noticed, prooving that $x(t)$ is a multifractal stationarity time series. The Figures B.2a and B.2b show the results of the generalized statistical function G_w for negative and positive values of w respectively.
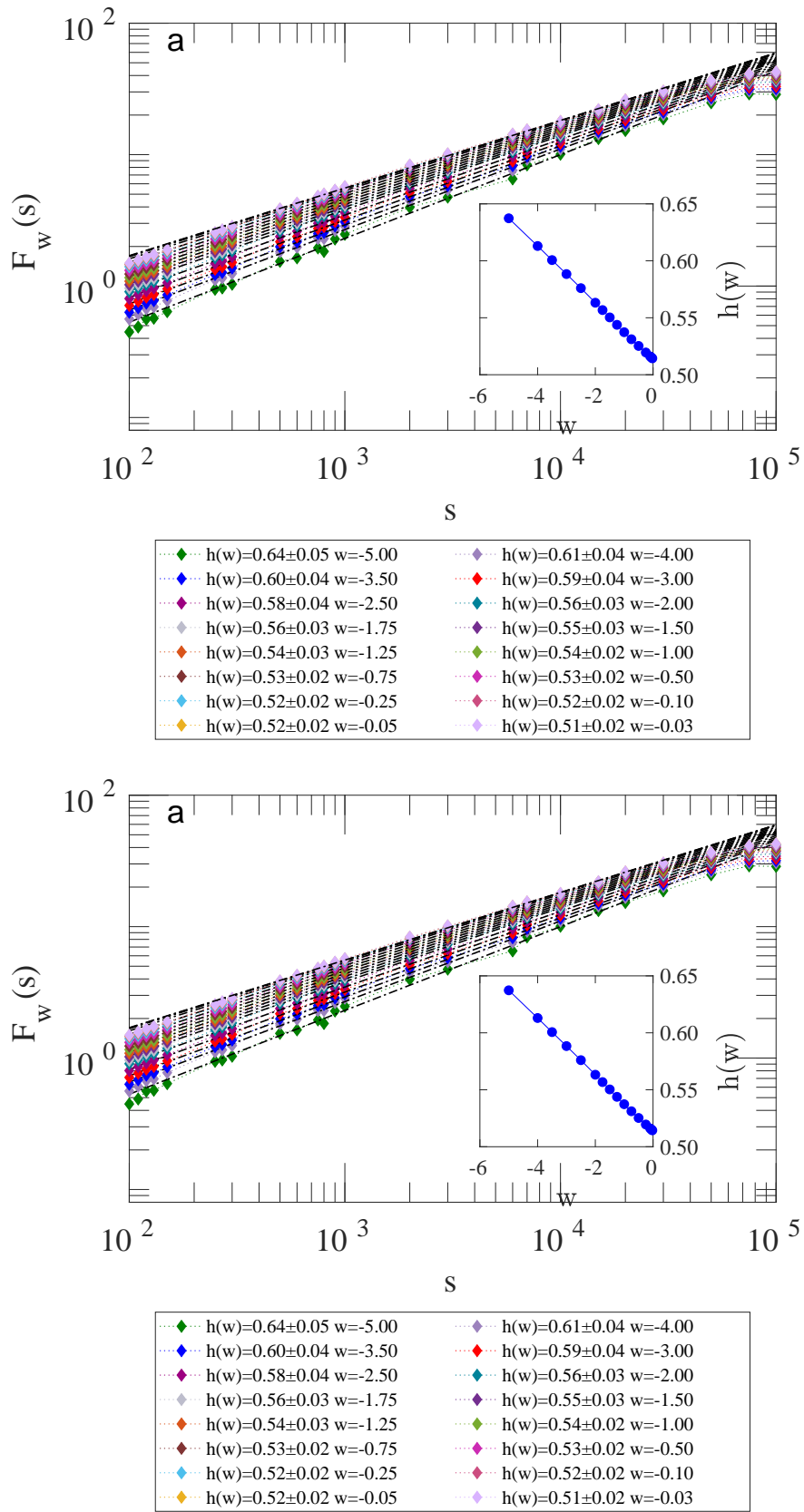
Figure B.1: Calculation of the statistical function F_w using Eq. (26). The function of F_w vs s display power laws $F_w(s) \sim s^{h(w)}$, where $h(w)$ depend on w. This feature demonstrates that the time series is a multifractal.
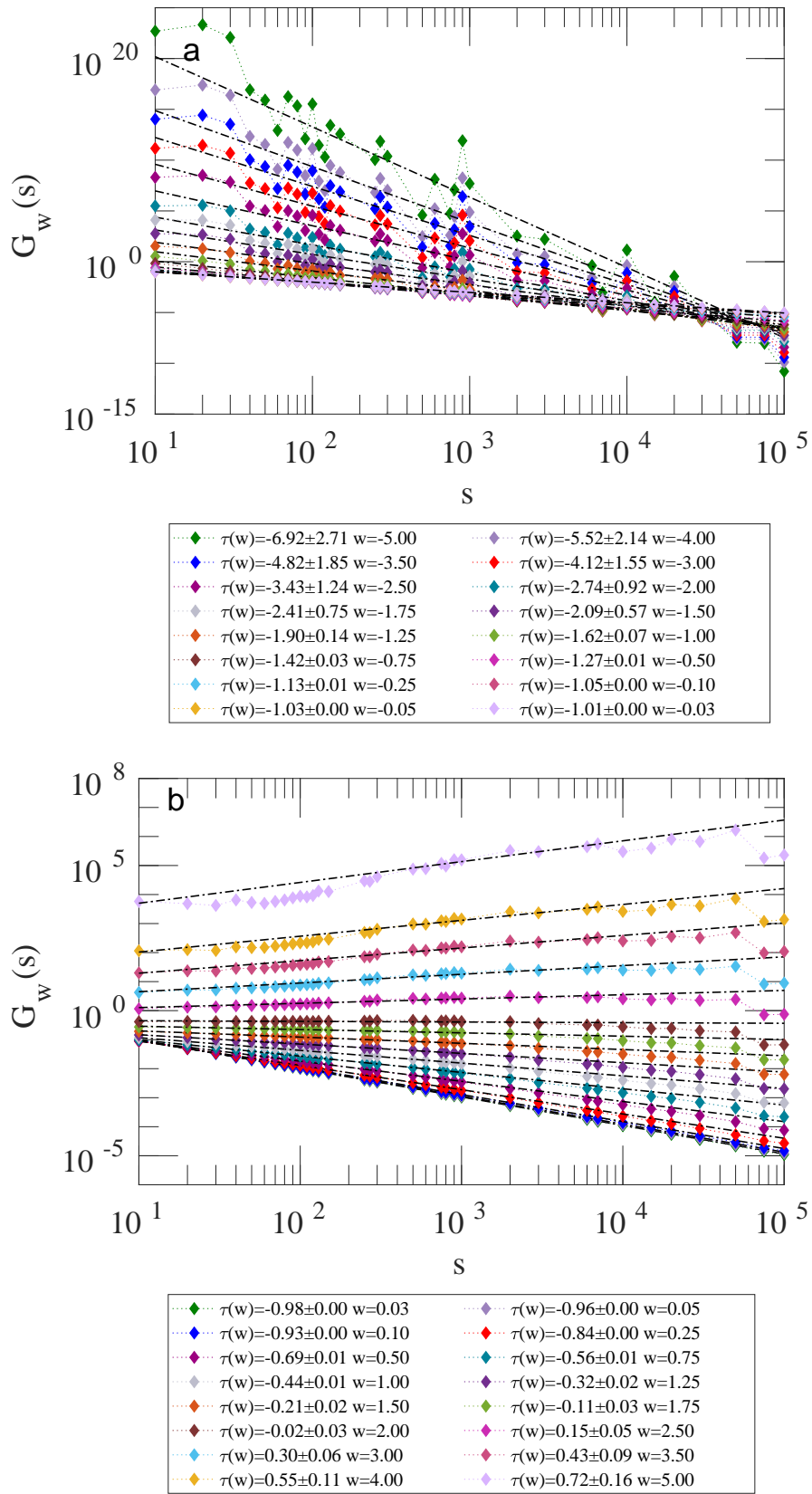
Figure B.2: Calculation of the "generalized statistical functions" $G_w(s)$ vs s for negative (a) and positive (b) values of order w. The "generalized statistical functions" is calculated by applying Eq. (31).